Atomic Force Microscopy for **Membrane Analysis:**

Membranes and filters are essential in all areas of manufacturing to assure purity and consistency of process. The atomic force microscope (AFM) offers a method for directly observing the three dimensional structure of membranes. AFM studies can be used for membrane development as well as monitoring membrane wear associated with use.

The purpose of this study is to simulate compressor contamination in industrial applications and to ascertain the behavioral changes in membranes over time with varying pollutant levels. Pereira and Admassu found that permeability was reduced in polymeric membranes-including poly(carbonate)-with an increase in oil contamination. Moreover, the selectivities of oxygen-nitrogen and methane-carbon dioxide mixes were improved. Several theories were proposed to account for the observed phenomena, and the recent AFM work provides topographical evidence for the manner in which the presence of oil altered the membrane surface structure.

Membrane Preparation

The poly(carbonate) samples mapped in this study were obtained from recent research on polymer membrane contamination.[1-3] Flat membranes were cast from a polymer solution prepared in methylene chloride and impregnated with various concentrations of oil. Poly(carbonate) membranes with oil concentrations of zero (clean), 10^3, 10^4, and 10^5 ppm were imaged, primarily with oscillating mode.

Experimental Results and Discussion

Dozens of poly(carbonate) membrane images have been analyzed at all four oil-contaminate levels over a variety of random locations and at multiple "magnifications." Only the most representative and enlightening ones are presented along with surface roughness statistics. Oscillating mode was employed for all image generation. Since the polymers were cast on float glass slides, the top surface exposed to air was expected to reveal marked differences compared to the bottom surface cast against the glass. Membrane films also tend to curl away from the bottom side when drying. This identification method is by no means fail-safe and results in the necessity of careful sample labeling, especially for clean polymer samples.

Several different length scales were examined for both sides of the membranes. The underside of all membranes was nonporous and relatively smooth, modeling the float glass surface. Because of this similarity, all images of membrane undersides were lumped together for analysis. No statistical differences of the underside were found for varied oil contamination or over image ranges from 30 mm to 50 mm on a side; the surface deviations are constant over this range. The 95% confidence interval for the overall average RMS roughness of the undersides was 23.4 ± 3.8 nm after linear flattening of 36 images.

It must be pointed out that one or two images in each batch were discarded as outliers. These were eliminated by falling outside of the raw mean by more than five standard deviations; all of these images had RMS roughness of the order of 100 nm and had clearly visible defects that were not representative of the polymer cast against smooth glass. If the area of interest for taking roughness measurements were on the millimeter scale, these features would not be justification for outlier elimination. Here, we are focusing on the microstructure only, not the effects of dirt contamination, crazes, and cracks.

It was initially thought that the RMS roughness of the bottom side would tend to be lower than the top, providing a quantitative basis for assisting in the differentiation of the top and bottom sides. While it is obvious from the images and visual inspection that oil contamination increased surface roughness, the variability in RMS was not consistent. The 95% confidence intervals for membrane topside roughness after linear flattening are 73±20 nm (clean membranes - 42 images), 33±8 nm (10^3 ppm oil - 16 images), 40±22 nm (10^4 ppm - 8 images), and 75±17 nm (10^5 ppm - 26 images). Values of RMS roughness based on ~10´10 mm2 images are 3.4±1.8 nm (clean - 18 images), 16.2±6.3 nm (10^3 ppm - 20 images), 7.4±0.9 nm (10^4 ppm - 18 images), & 117±40 nm (10^5 ppm - 20 images).

These collective data indicate statistical differences in the membrane batches. However, it is unclear why the supposedly clean membrane was essentially as rough as the most highly oil-contaminated membrane. For large AFM images, the trend of increasing roughness for 10^3, 10^4, & 10^5 ppm is real but not sufficient for a blind study. This is supported by the lack of consistent trend in the smaller images. Most importantly, the apparent discrepancies imply that there are other factors of importance. Ultimately, roughness values alone are not a sufficient means of sample classification for this experiment and must be approached with caution in any study.

The individual images must be examined for further insight into structural property effects from oil, and this is where the more interesting data are found. During the membrane drying stage, solvent escapes into the air and roughens the topside. This also aids the migration of oil toward the free surface. On the macroscopic scale, the higher contamination levels (e.g., 10^5 ppm) appear cloudy and dull to the unaided eye, while the bottom side is glossy. Scans of the 10^5 ppm oil-contaminated membranes revealed numerous pits of 0.5 to 1.5 µm (Fig. 1) responsible for the dull appearance, due to light scattering.

Figure 1

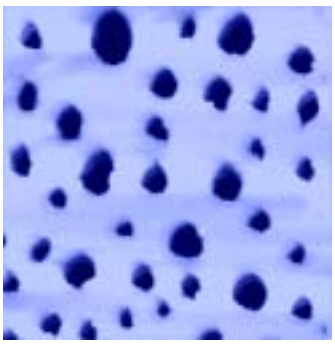

10^5 ppm membrane, raw scan at 9.7 x 9.7 mm^2; RMS roughness is 105 nm.

The 10^4 ppm samples also displayed the pitted effect but to a lesser degree, with pits approximately 100 nm in diameter and much more numerous (Fig. 2).

Figure 2

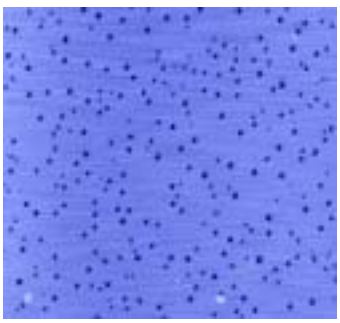

10^4 ppm membrane, raw scan at 9.7 x 9.7 mm^2; RMS roughness is 7.11 nm.

The pits were notably smaller than at the 10^5 ppm level, possibly indicating differences in oil solubility in polymer solution or the decreasing probability of oil droplet coalescence at lower volume fractions. Figures 3 and 4 show cross-sectional views for the 10^5 and 10^4 ppm oil concentrations, respectively, and provide an extended comparison of crater dimensions.

Figure 3

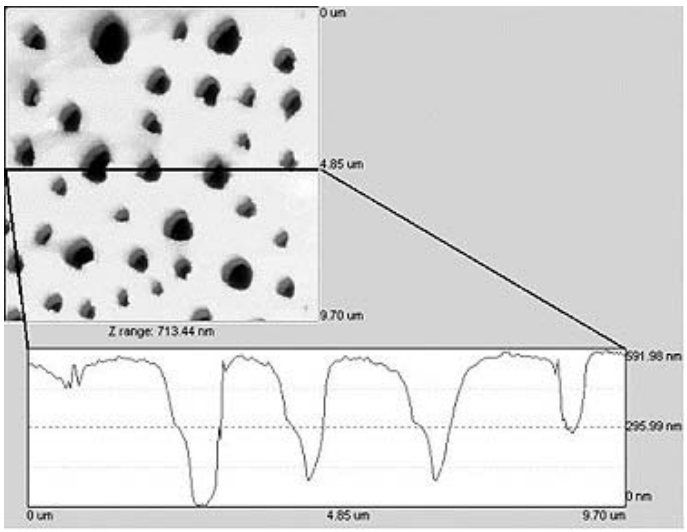

10^5 ppm membrane, raw scan at 9.7 x 9.7 mm^2 and cross section of pits.

Figure 4

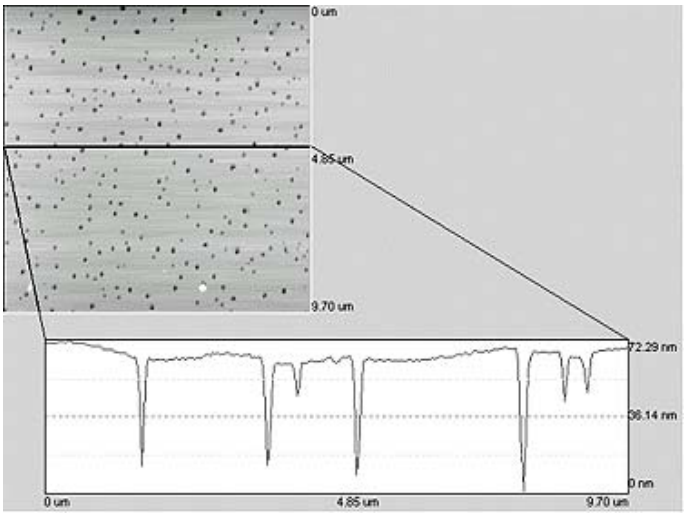

10^4 ppm membrane, raw scan at 9.7 x 9.7 mm^2 and cross section of pits

The holes at 10^5 ppm appear to be an order of magnitude wider and deeper than those at 10^4 ppm. However, the nature of AFM skews the depth observation. Since the AFM probe tip is conical-sometimes pyramidal-in shape, it cannot access very narrow or deep features. Therefore, we can

only accurately measure diameter at the surface and glean minimum crater depths from the images.

Craters were also discovered in the 10^3 ppm doping (Fig. 5) with much less frequency and of similar size to those at 10^4 ppm.

Figure 5

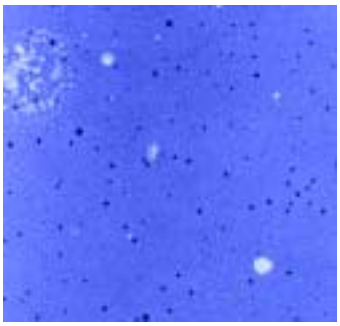

10^3 ppm membrane at 5 x 5 mm^2 scale; RMS roughness is 3.94 nm.

Figure 5 begins to reveal the source of what might be considered the true polymer roughness at the nanometer scale. The larger, high (white) features reveal the level of non-oil contaminant (i.e., dirt). Small bumps only 1-5 nm high are resolved at this scale in the relatively clean regions between craters. This is coming near the noise threshold of these scanning conditions. The clean membrane consistently showed a lack of significant features for various resolutions, from square images of 4 to 80 µm over several sample locations.

Conclusion

This study shows the power of AFM for studying the effects of contamination on polycarbonate membranes. The advantage of the AFM is its capability to directly measure three dimensional images of membrane structure.

** This study is abstracted from a paper in progress by G.R. Stone and D.E. Aston. Image processing was performed with a MATLAB® m-file written to clean up the raw data with independent line-by-line flattening, excluding outlying points, such as dirt and pits.*

References

1. Pereira, B.; Admassu, W. "Effects of Chemical Impurities on Gas Sorption in Polymeric Membranes. I. Polycarbonate and Polysulfone." Sep. Sci. Technol. 2001, 36, 177-197.

2. Pereira, B.; Admassu, W.; Jensvold, J. "Effects of Chemical Impurities on Gas Sorption in Polymeric Membranes. II. PC-1 and PC-2." Sep. Sci. Technol. 2001, 36, 417-42.

3. Pereira, B.; Admassu, W.; Jensvold, J. "Effects of Chemical Impurities on Gas Permeation and Diffusion in Polymeric Membranes." Sep. Sci. Technol. 2001, 36, 3121-40.